1   Introduction

During the laboratory experiment, an FTIR spectrometer has been utilized to carry out a series
of precise measurements. The first task was to gather spectral data from the laboratory that
could be further analyzed to extract valuable information about the experiment. Following the
experimental phase, data was then processed using Python scripts, which allowed the calibration
of the instrumentation and the generation of a variety of informative plots and results about
various surface temperatures and ammonia concentrations.

2   Experimental Setup

During the laboratory, we have been provided with a FTIR spectrometer (Figure 1). It is an
instrument that uses infrared light and an interferometer to generate a detailed spectrum of a
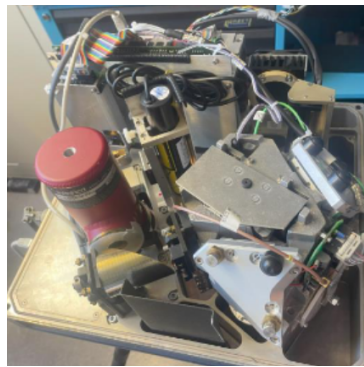sample's chemical composition.

Figure 1: Used FTIR spectrometer

The FTIR spectrometer works thanks to a Michelson interferometer (Figure 2). It splits an
infrared beam into two paths using a beam splitter (the mirror in the middle), with one path
being reflected by a moving mirror. As the mirror moves, the interference pattern it creates (an
interferogram) contains information about all the wavelengths in the beam. This interferogram is
then converted into a spectrum using Fourier transformation. It allows for faster data acquisition,
higher sensitivity, and better spectral resolution compared to traditional methods.
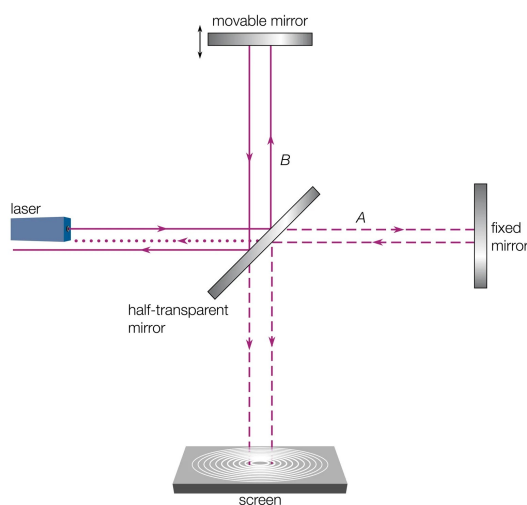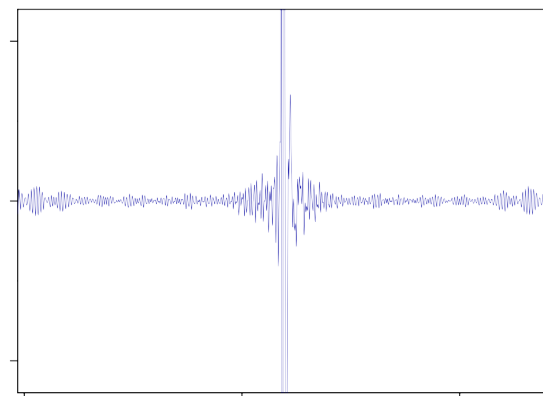

Figure 2: Michealson interferometer

Figure 3: A typical interfereogram graph

As it can be seen from the image below (Figure 4), the instrumentation was cooled down with liquid nitrogen in order to avoid self generated noise.

Figure 4: Intrumentation cooling down

As measured sources we use at first a flat black body inside the FTIR to calibrate the instrumentation (see Section 3.1.1 and 3.1.2), on which five different temperature were imposed using the given software.

Then we measured the emission spectra of five different surfaces: Stomach, Sky, interior room wall, exterior wall and an additional surface that was a black roof exposed to light. Starting from the obtained spectra we were asked to retrieve each single temperature, to accomplish this task we choose to use a least square approach (see Section 3.2).

Finally, we were asked to estimate the concentration of ammonia inside the measurement cell (Figure 5), using it as a "cloud" in between different background: stomach and sky.

Figure 5: Ammonia bucket

3 Methods and Results

3.1 Instrumentation Calibration

In the following sections, we will discuss the first step in processing the collected data: instrumentation calibration. The data acquired consists of a series of raw spectra derived from various black-body sources, which currently do not provide a clear interpretation of the y-axis. We will address this challenge and present the corresponding solution in the following discussion.

3.1.1 Black Body measures

The initial step was to measure the blackbody emission from an object that closely simulates a true blackbody at five distinct temperatures: 273K, 293K, 313K, 343K, and 352K. The instrumentation has been cooled down with nitrogen to remove source noises. The figure on the left (Figure 6) shows the raw spectrum obtained from the measurement, while the one on the right (Figure 7) presents the spectrum after filtering out noise caused by air absorption between the sensor and the blackbody. The filter has been implemented using a moving average to prevent division by zero during the calculation of slopes and offsets in the next steps.
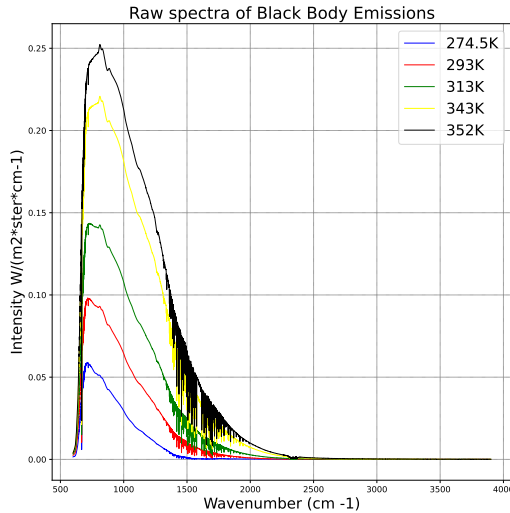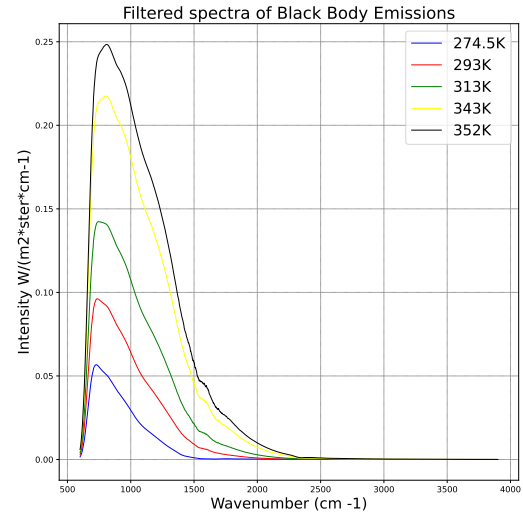
Figure 6: Raw measure with noise   Figure 7: After filtering for air absorption

3.1.2 Radiometric calibration

After plotting the raw spectra, we need to assign the correct units of measure to the intensity, as it has been recorded in arbitrary digital units. We were provided with the following formula to calculate meaningful quantities, considering that the instrument has a linear response to radiance.

$$I_{calibrated}(v, T) = slope(v) \cdot I_{measured} + offset(v)$$

To compute the slope and offset, we need at least two measured spectra and the respective theoretical one to form a system of two equations with two unknowns. The theoretical ones

were computed using the black-body formula:

$$B(v, T) = A \cdot \Omega \cdot \frac{c_1 \cdot v^3}{e^{\left(\frac{c_2 \cdot v}{T}\right)} - 1}$$

As shown in our Python code, we determined the slope by analyzing four pairs of spectral measurements (273K and 293K; 313K and 343K; 273K and 313K; 273K and 343K) and then averaging the resulting slope and offset values.

Once we have obtained these values, we computed the theoretical emission spectra of the $T_5 = 352K$ measurements (in black) and we compared it with the calibrated one (in green) as shown below (Figure 8), in order to verify the functioning of the calibration.
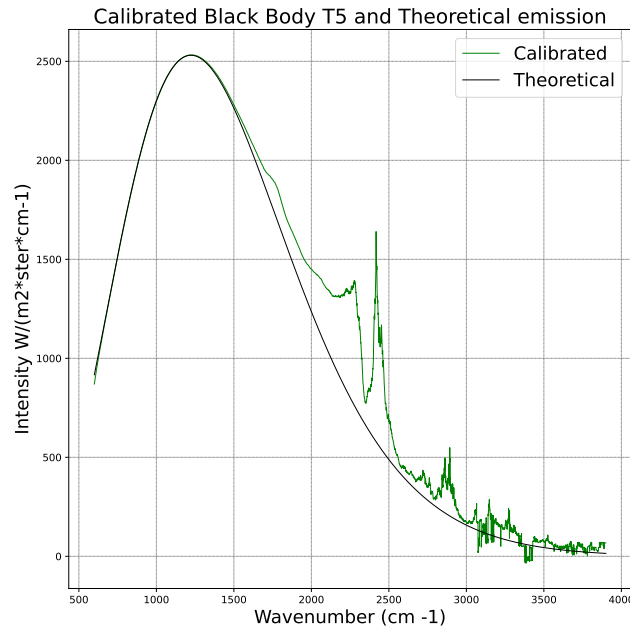

Figure 8: Calibrated T5 spectra compared with Theoretical Black body T5 emission

Numbers beyond 2000 cm^{-1} are not so relevant as they do not represent clear information since the measured IR intensity starts not to emit light and are not useful for our next steps (Section ??) because ammonia absorption is generally observed around 950–1100 cm^{-1}.

3.2 Temperature Retrivial

As presented in the previous sections, after calibrating the instrumentation, we were tasked with determining the temperature values for several spectral measurements: the stomach, the sky, the interior wall of a room, the exterior wall, and an additional surface that was a black roof exposed to light.

To obtain temperature measurements, the least squares method has been utilized to optimize the temperature parameter T. This approach seeks to ensure that the black body model fits the measured data accurately, employing the following mathematical framework:

$$residual = \sum_i (I_{measured} - black\_body(x, T))$$

In the figure below (Figure 9), is represented our Python function used to accomplish this task.

```python
from scipy.optimize import least_squares

def residuals(param, x_axes, I):
    T = param
    return I - black_body(x_axes, T)

def temperature_fitter(x_axes, I_calibrated):
    initial_guess = 293
    result = least_squares(residuals, initial_guess, args=(x_axes, I_calibrated))
    fitted_T = result.x[0]

    return fitted_T

fitted_T = temperature_fitter(I_calibrated_352K[:, 0], I_calibrated_352K[:, 1])

print(f"fitted T: {fitted_T}")
```
✓ 0.0s

Figure 9: Fitting Script algorithm in Python

The function "residuals" computes the difference between the measured intensity I and the intensity predicted by the black body model for a given temperature T. These differences (or residuals) represent the errors between the model and the actual measurements.

The function temperature_fitter starts with an initial guess for $T = 293K$ and then calls "least_squares" from the scipy.optimize module. This function adjusts T to minimize the sum of the squares of the residuals.

Finally, applying the calibration from the previous step, and the fitting function to our new measurements, we found the following temperature values for our measurements:

- Stomach: 30.79°C

- Sky: 1.34°C

- Inside Wall: 19.92°C

- Outside Wall: 8.89°C

- Additional surface outside: 8.73°C

The results appear to align well with the expected values. The room temperature was approximately 20°C, while the outside temperature was around 1°C. It is likely that the outside walls had been exposed to sunlight, we have to take into consideration that they had been warmed also from the inside. This could explain the higher temperature compared to the outside temperature. Regarding the stomach temperature, we know that the typical human body temperature is around 36°C to 37°C. However, we measured it at around 31°C. This discrepancy can be attributed to the fact that the stomach is not a black body and that the surface temperature is typically lower than the internal body temperature.

3.3 Ammonia concentration retrievals

Now that we have verified the correct calibration of our spectra and measured some temperatures we proceed with measuring a concentration of ammonia in a gas sample. As explained in section 2, our sample is diluted in air inside a bucket with transparent sides that allow light to fully cross it.

As background, both the sky and the stomach were used. In total, four different spectra were measured (Figure 10): the spectra of the empty bucket with both backgrounds and the spectra of the bucket containing ammonia with both backgrounds.
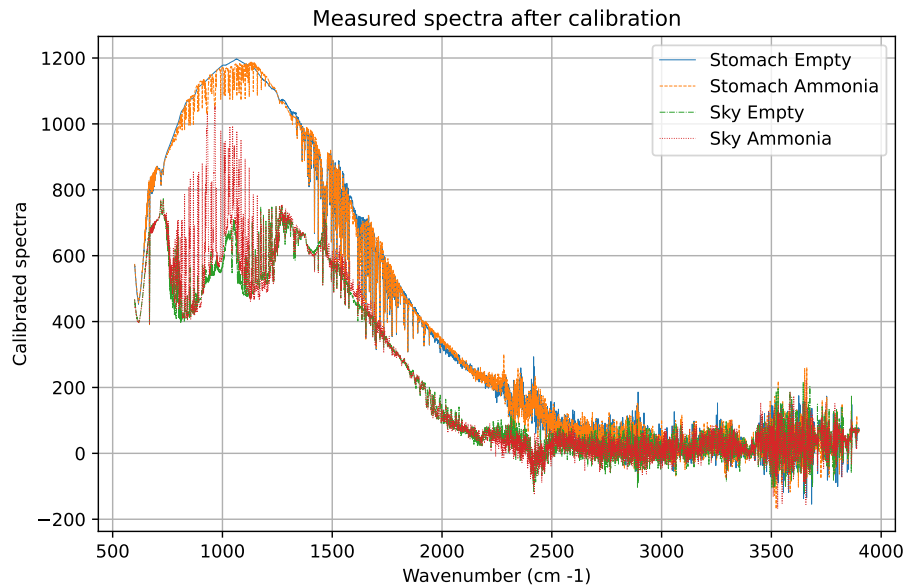

Figure 10: Measured and calibrated spectra

Before retrieving the concentration, further analysis of these spectra is required.

For wavenumbers above $2000cm^{-1}$, there is little light in the detector so the noise we see in the plot is of no importance. There is no information to be retrieved in those regions.

The orange and blue curves belong to the stomach background, there is a base line that is the blackbody radiation spectrum of the stomach.

The sample is colder than the background so the fingerprint presents spikes that extend down from the baseline.

The red and green curves belong to the sky background. As the sample is hotter than the background the spikes in turn extend upwards. It is important to notice as well that the baseline is not a blackbody curve and there are large gaps close to the $800cm^{-1}$ and to the $1200cm^{-1}$ due to the gases in the sky, especially CO_2 and O_3.

To obtain the concentration of ammonia from these spectra, we use the ammonia effective cross section, a fundamental parameter of the Beer-Lambert law. We were supplied with the absorbance of ammonia at $100ppm = 10^{-4}$(volume fraction), 293K , atmospheric pressure and

length x = 1m. From the perfect gas law we derive the formula:

$$\sigma(\nu) = A(\nu)\frac{1}{\frac{P}{k_B T} \cdot 10^{-4} \cdot x \cdot log_{10}(e)} \approx A(\nu) \cdot 9.31465109174741 \cdot 10^{-22} \tag{1}$$
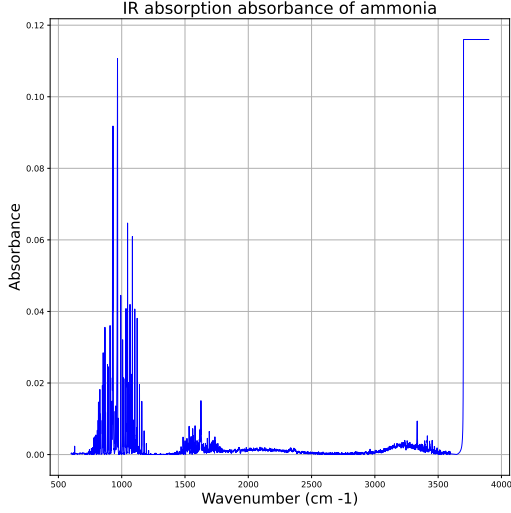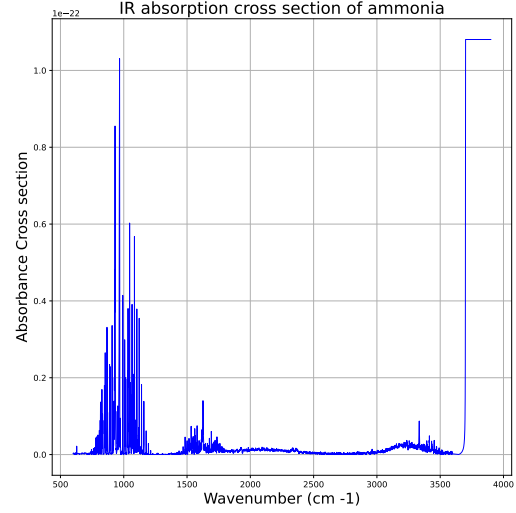

Figure 11: Ammonia absorbance

Figure 12: Ammonia Cross Section

The model we use is based on the Beer-Lambert law. If c is the concentration in molecules per volume, the intesity of light that crosses a distance x of a substance will come out multiplied by t_{cloud}:

$$t_{cloud} = e^{-\sigma(\nu) \cdot x \cdot c} \tag{2}$$

$$I_{obs} = I_{background} \cdot t_{cloud} + B_{cloud} \cdot (1 - t_{cloud}) \tag{3}$$

$$t_{cloud} = \frac{I_{obs} - B_{cloud}}{I_{background} - B_{cloud}} \tag{4}$$

$$c_{cloud} = \frac{-1}{\sigma(\nu)x_{cloud}} \cdot ln(t_{cloud}) \tag{5}$$

t_{cloud} is the transmittance of the cloud. It is function of wavelength and is from it we can retrieve concentrations. It should less than 1 because when light crosses the gas cloud it cannot gain intensity. Notice how we use $I_{background}$ instead of the usual $B_{background}$. This is because we use the measured background spectrum instead of a theoretical blackbody curve for this term.
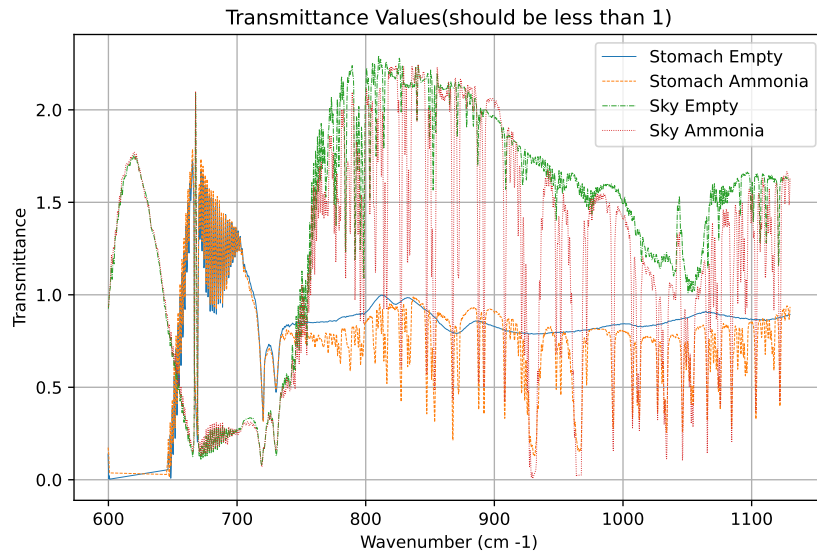
Figure 13: Transmittance using theoretical black bodies

The results above (Figure 13) are obtained when the transmittance formula is blindly applied with blackbody radiation curves for the subtracting terms.
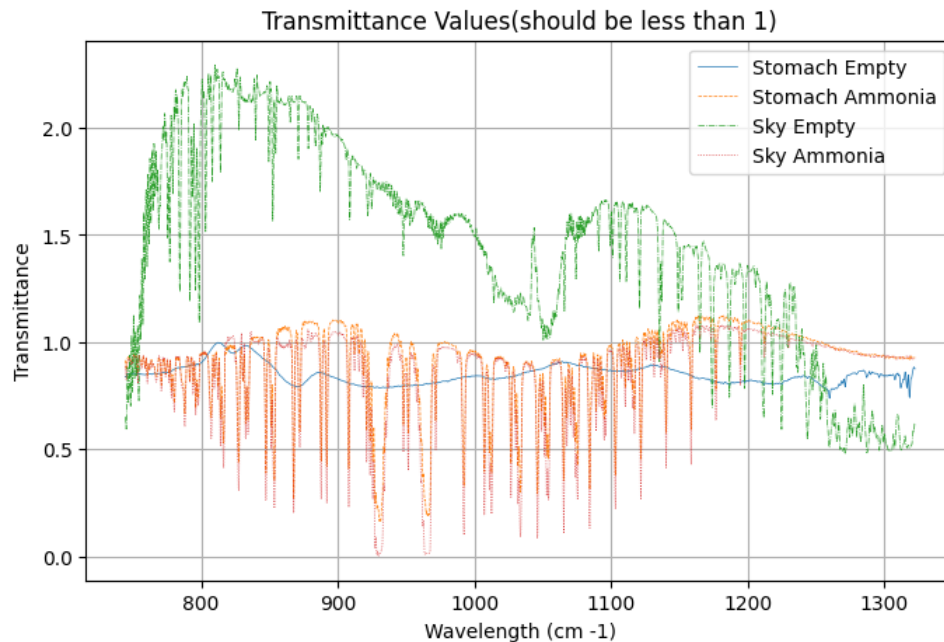

Figure 14: Transmittance using measured background

Figure 14 instead shows the corrected transmittance for the bucket containing ammonia. Logically, the control transmittances cannot be corrected as they lack their own control. Notice that the orange and red curves, which represent the ammonia samples, are nearly identical and remain between 0 and 1. This result is expected since it is the same sample measured with different backgrounds.

There are however some differences. Table 1 presents values read from the plots for finding the concentration.

Wavenumber (cm^{-1})	$t_{\text{cloud,stomach}}$	$t_{\text{cloud,sky}}$	Cross-section (m^2)
932	0.2096727	0.027152	6.127×10^{-23}
967	0.1939230	0.016415	1.031×10^{-22}

Table 1: Point values for concentration calculation

We apply equation (5) which gives a concentration value per transmittance/cross-section pair at table 2:

Wavenumber (cm^{-1})	$c_{\text{cloud,stomach}}$ (m^{-3})	$c_{\text{cloud,sky}}$ (m^{-3})
932	9.8066×10^{22}	2.26381×10^{23}
967	6.1209×10^{22}	1.5335×10^{23}

Table 2: Concentration values from pointwise calculation

The average value of the concentration is 1.347×10^{23} molecules m^{-3}.
To convert back to volume fraction we use the perfect gas law $V/V = c\frac{k_B T}{P}$, which in our conditions gives $V/V \approx 0.55\%$.
This was the point wise method. Another way to obtain the concentration is to use the two wavenumbers measurements together like shown in equation (7):

$$\frac{t(\nu_1)}{t(\nu_2)} = \frac{exp(-\sigma(\nu_1)xc)}{exp(-\sigma(\nu_2)xc)} = exp(-(\sigma(\nu_1)xc + \sigma(\nu_2)xc) \tag{6}$$

$$c = \frac{-1}{(\sigma(\nu_1) - \sigma(\nu_2))x} ln\left(\frac{t(\nu_1)}{t(\nu_2)}\right) \tag{7}$$

The average between the sources gives $c = 2.674 \times 10^{21} m^{-3}$, $V/V \approx 108.5 ppm = 0.0108\%$.

This second method usually is done with spectra ratio instead of transmittance but this way no approximation is needed.

The methods shown can be averaged over a band of wavenumbers of course but each point in the spectra enters into consideration independently. The final method used is the strongest and is by fitting the spectrum.

The idea is that the transmittance measured does not belong only to ammonia but to a variety of substances. To remove them we consider a cascade of transmittances, each multiplying the light intensity after the other. The absorbances, logarithms of the transmittance, add up in a linear combination.

$$A_{total} = \sum A_i = \sum \sigma_i \cdot x \cdot c_i \cdot log_{10}(e) \tag{8}$$

By doing a linear regression we can write the measured absorbance as a weighted sum of cross-sections. The weight we find for the ammonia cross-section will be $weight_{NH_3} = x \cdot c_i \cdot log_{10}(e)$.
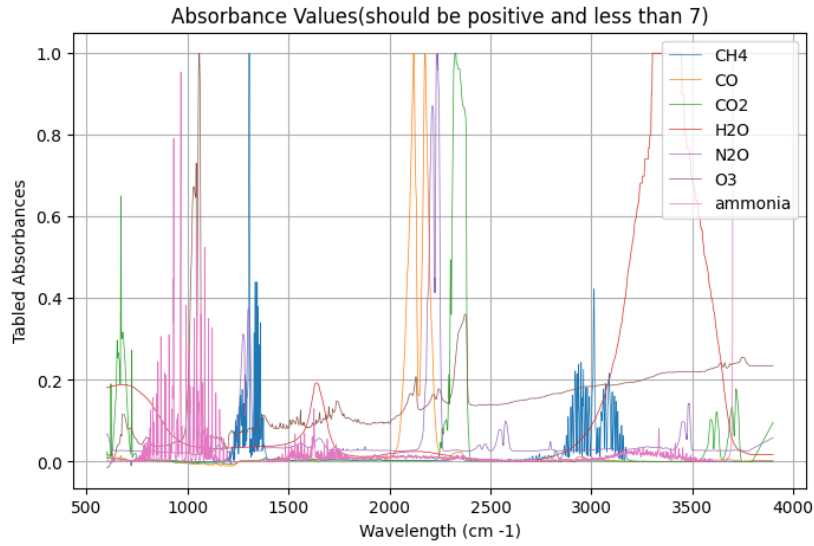
Figure 15: Normalized cross sections for fitting

In Figure 15 we present once again the ammonia cross-section along with others from different substances (H_2O, CO_2 ...) retrieved from the internet (NIST Chemistry WebBook, US Department of Commerce). All cross-sections were interpolated to fit the same horizontal scale and normalized to facilitate the fitting. The actual values of the cross-sections, besides the ammonia one, are irrelevant as only their shape is required. The normalization factor for the ammonia was its maximum, that is, $1.0804995266426996 \times 10^{-22} m^2$.

As we know that ammonia only has an active infrared cross section between roughly $900cm^{-1}$ and $1000cm^{-1}$ we restrict the fitting to this region. For the fitting algorithm, we use a simple linear regression with a small regularization term to avoid overfitting (Ridge regression), that is, fitting noise.
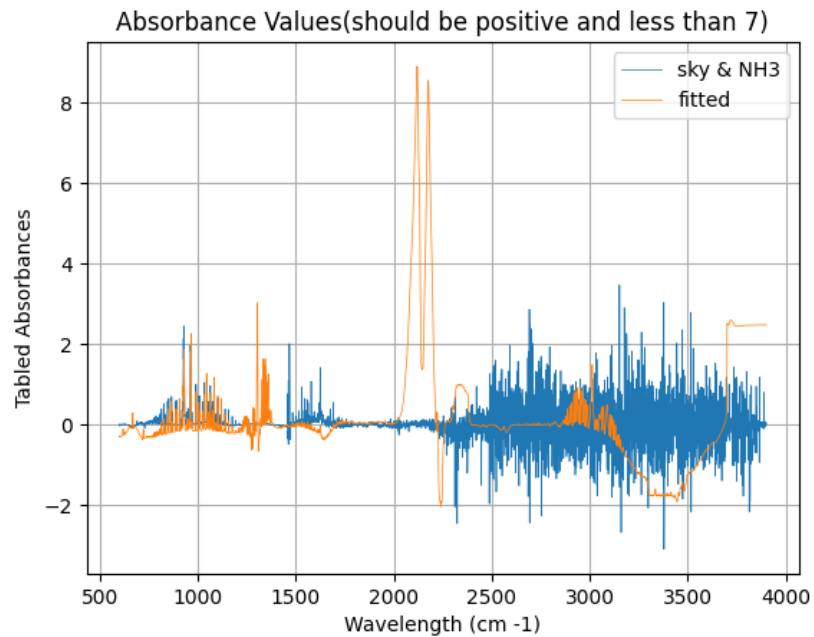

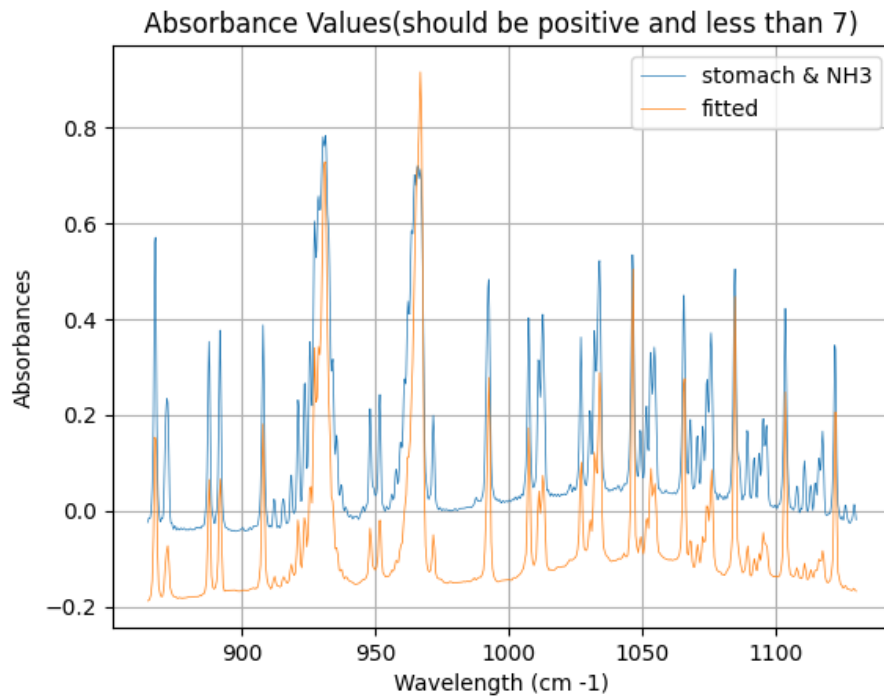Figure 16: Fitted absorbance plotted for all wavenumbers

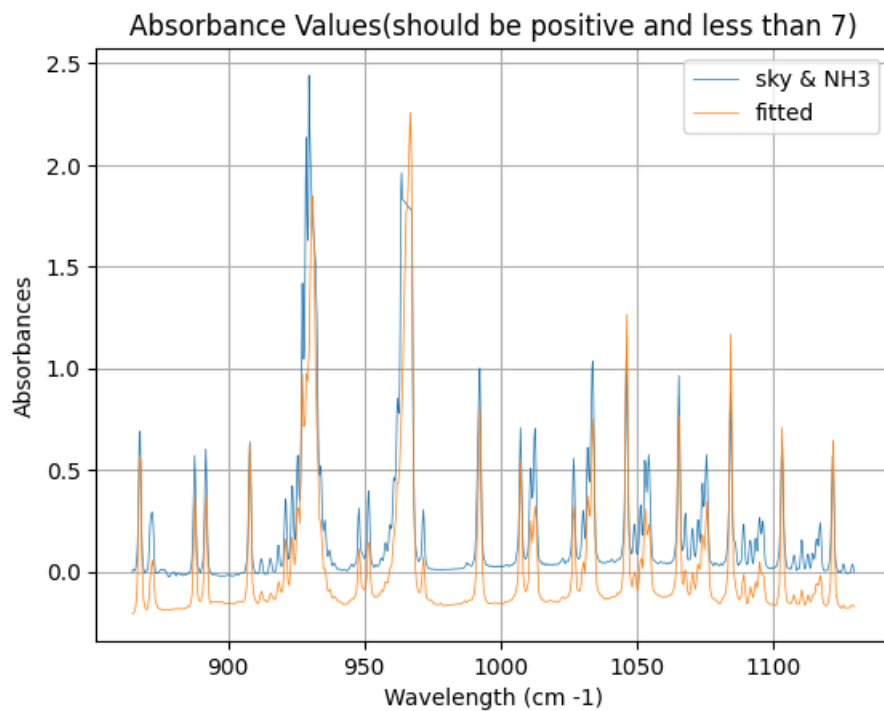Figure 18: Fitted absorbance in area of fit (stomach background)

Figure 17: Fitted absorbance in area of fit (sky background)

As expected, when the fitted absorbance is plotted for all wavenumbers, it appears significantly different from the measured values. However, for the selected area, the correlation coefficients are $r^2 = 0.8924$ for the sky background and $r^2 = 0.8892$ for the stomach background. These values are notably high, as they are close to 1, which indicates a perfect fit.

The weights are $weight_{sky} = 2.528882$, $weight_{stomach} = 1.11661415$. As the cross sections had been normalized we must correct for it which leads to:

$$weight = x \cdot \sigma_{max} \cdot c \tag{9}$$

$$c = weight \cdot \frac{weight}{\sigma_{max} \cdot x} \tag{10}$$

By plugin in the previous values this results in $c_{sky} = 9.006 \times 10^{22} m^{-3}$, $V/V_{sky} \approx 0.365\%$, $c_{stomach} = 3.9765 \times 10^{22} m^{-3}, V/V_{stomach} \approx 0.1613\%$. If we average we get a final result:

$$c_{NH_3} = 6.49125 \times 10^{22} m^{-3} \tag{11}$$

$$V/V_{NH_3} = 0.263\%$$

4   Discussion

After processing the raw data obtained during our laboratory measurements, our analysis confirmed the anticipated outcomes. The calibrated spectra closely match the theoretical predictions, and the least squares fitting of the blackbody curves produced temperature values in good agreement with our set points.

As it can be seen, the most challenging part was to retrieve ammonia concentration from our data. At the end, the spectral features corresponding to gas absorption and emission were identifiable and consistent with the literature.

This data processing approach we had, can validate our experimental setup and methodology and also reinforces our understanding of the reliability of the FTIR technique for precise spectral analysis.